RESEARCH ARTICLE

ER Quality Control Components UGGT and STT3a Are Required for Activation of Defense Responses in *Bir1-1*

Qian Zhang, Tongjun Sun, Yuelin Zhang*

Department of Botany, University of British Columbia, Vancouver, Canada

* yuelin.zhang@ubc.ca

Abstract

The receptor-like kinase SUPPRESSOR OF BIR1, 1 (SOBIR1) functions as a critical regulator in plant immunity. It is required for activation of cell death and defense responses in Arabidopsis *bak1-interacting receptor-like kinase 1,1* (*bir1-1*) mutant plants. Here we report that the ER quality control component UDP-glucose:glycoprotein glucosyltransferase (UGGT) is required for the biogenesis of SOBIR1 and mutations in *UGGT* suppress the spontaneous cell death and constitutive defense responses in *bir1-1*. Loss of function of *STT3a*, which encodes a subunit of the oligosaccharyltransferase complex, also suppresses the autoimmune phenotype in *bir1-1*. However, it has no effect on the accumulation of SOBIR1, suggesting that additional signaling components other than SOBIR1 may be regulated by ER quality control. Our study provides clear evidence that ER quality control play critical roles in regulating defense activation in *bir1-1*.

Introduction

Eukaryotic cells have evolved several quality control mechanisms to monitor the folding of secretory proteins in the endoplasmic reticulum (ER) [1,2]. Correctly folded proteins are allowed to export to their final destinations, whereas misfolded proteins are retained in the ER for additional folding process or degraded by the ER-associated degradation pathway.

One of the well-studied protein folding pathway specific for secreted glycoproteins is the calnexin (CNX)/calreticulin(CRT) cycle, which involves ER-localized lectin-like chaperones CNX/CRT and the UDP-glucose:glycoprotein glucosyltransferase (UGGT) [3]. Following protein translation, preassembled glycan chains ($Glc_3Man_9GlcNAc_2$) are transferred to the Asn (N)-residues in the N-X-Ser/Thr sequences in acceptor proteins by the oligosaccharyltransferase (OST) complex. Trimming of two glucose residues from the glycan chain by glucosidases generates proteins with monoglucosylated glycans ($GlcMan_9GlcNAc_2$), which CNX and CRT interact with and assist with folding in the ER. Subsequent removal of the remaining glucose from $GlcMan_9GlcNAc_2$ leads to dissociation of the client protein from CNX and CRT. Proteins that attained their nature structure can then enter the secretory process, whereas improperly folded proteins are recognized by UGGT and a glucose residue is added back to the

$Man_9GlcNAc_2$ by the enzyme. The monoglucosylated proteins subsequently associate with CNX and CRT to go through another round of folding.

UGGT and CRT3 have been shown to play important roles in the biogenesis of transmembrane receptors in plants. Retention of the defective brassinosteroid receptor bri1–9 protein in the ER requires both UGGT and CRT3 [4,5]. In Arabidopsis *uggt* and *crt3* mutant plants, accumulation of the receptor-like kinase (RLK) EFR, which recognizes bacterial EF-Tu, is reduced [6,7]. Expression of the tobacco protein INDUCED RECEPTOR-LIKE KINASE was also shown to be dependent on NbCRT3 [8]. In tomato, silencing of CRT3a affects the biogenesis of Cf-4 and leads to loss of pathogen resistance mediated by Cf-4 [9]. In addition, loss of function mutations in Arabidopsis *STT3a*, which encodes the catalytic subunit of the OST complex, also cause reduced EFR protein level and impair its function in plant immunity [7,10].

In Arabidopsis, BAK1-INTERACTING RECEPTOR-LIKE KINASE 1 (BIR1) negatively regulates cell death and defense responses mediated by the RLK SOBIR1 (SUPPRESSOR OF BIR1, 1) [11]. Previous studies showed that activation of defense responses in *bir1–1* is also dependent on the β and γ subunits of heterotrimeric G protein as well as several ER quality control (ER-QC) components including CRT3, ERdj3b and SDF2 [12,13]. Here we report that additional ER-QC regulators, UGGT and STT3a, also play important roles in the regulation of defense responses in *bir1–1*.

Results and Discussion

Identification and characterization of *sobir6–1 bir1–1 pad4–1*

To identify defense pathways activated in *bir1–1*, a suppressor screen was carried out in the *bir1–1 pad4–1* mutant background [11]. *sobir6–1* is one of the mutants identified from the screen. In the *sobir6–1 bir1–1 pad4–1* triple mutant, the dwarf morphology of *bir1–1 pad4–1* is almost completely suppressed (Fig. 1A). Analysis of the expression levels of defense marker genes *PATHOGENESIS-RELATED 1* (*PR1*) (Fig. 1B) and *PR2* (Fig. 1C) in *sobir6–1 bir1–1 pad4–1* showed that *PR2* expression is significantly lower than in *bir1–1 pad4–1*. In addition, *sobir6–1 bir1–1 pad4–1* supports much higher growth of the oomycete pathogen *Hyaloperonospora arabidopsidis* (*H.a.*) Noco2 than *bir1–1 pad4–1* (Fig. 1D). These data indicate that the constitutive defense responses observed in *bir1–1 pad4–1* is largely suppressed by *sobir6–1*.

SOBIR6 encodes UGGT

The *sobir6–1* mutation was mapped to a region between marker T2E12 and T8K14 on Chromosome 1 using a mapping population generated by crossing *sobir6–1 bir1–1 pad4–1* (in the Columbia ecotype background) with Landsberg. Further fine mapping analysis narrowed the mutation to a 70 kb region between markers F23N20 and F26A9 (Fig. 2A). To identify the *sobir6–1* mutation, PCR fragments covering this region were amplified from genomic DNA of *sobir6–1 bir1–1 pad4–1* and sequenced. A single G to A mutation was identified in *AT1G71220*, which encodes the ER-QC component UGGT. The mutation is located at the junction between the 29th intron and 30th exon of *UGGT*.

In the same mutant screen, we also identified two additional alleles of *sobir6*. Both of them failed to complement *sobir6–1* (Fig. 2B). Sequence analysis of *UGGT* in *sobir6–2* and *sobir6–3* showed that they also contain mutations in the gene. In *sobir6–2*, a C to T mutation changes Ala_{1426} to Val. In *sobir6–3*, a G to A mutation introduces a stop codon in the coding region (Fig. 2C). These data suggest that *SOBIR6* is *UGGT*.
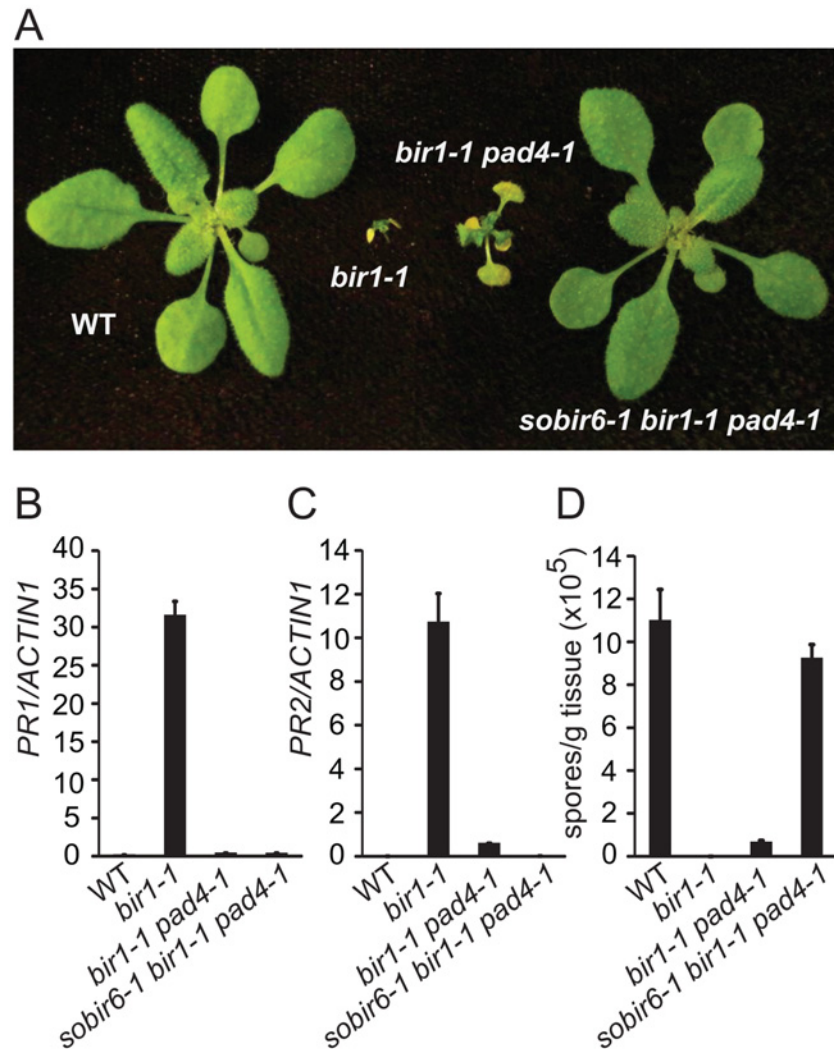
Fig 1. Characterization of the *sobir6–1 bir1–1 pad4–1* triple mutant. (A) Morphology of Col-0 wild type (WT), *bir1–1*, *bir1–1 pad4–1* and *sobir6–1 bir1–1 pad4–1*. Plants were grown on soil at 23°C and photographed three weeks after planting. (B-C) Expression levels of *PR1* (B) and *PR2* (C) in WT, *bir1–1*, *bir1–1 pad4–1* and *sobir6–1 bir1–1 pad4–1* seedlings compared to *ACTIN1*. Total RNA was extracted from 12-day-old seedlings grown on half-strength MS plates. (D) Growth of *H. a*. Noco2 on WT, *bir1–1*, *bir1–1 pad4–1* and *sobir6–1 bir1–1 pad4–1* seedlings. Error bars in (B-D) represent standard deviations of three measurements.

doi:10.1371/journal.pone.0120245.g001

UGGT is required for constitutive defense responses in *bir1–1*

To test whether *sobir6–1* can suppress the constitutive defense responses in *bir1–1* in the absence of *pad4–1*, we isolated the *sobir6–1 bir1–1* double mutant from the F2 population of a cross between *sobir6–1 bir1–1 pad4–1* and wild type. *sobir6–1 bir1–1* is much bigger than *bir1–1*, but smaller than wild type (Fig. 3A). In *sobir6–1 bir1–1*, expression of both *PR1* and *PR2* is greatly reduced compared to that in *bir1–1* (Fig. 3B-C). As shown in Fig. 3D, resistance to *H.a*. Noco2 is also considerably reduced in *sobir6–1 bir1–1*. These data suggest that UGGT is required for the constitutive defense responses in *bir1–1*. This is consistent with the requirement of another component of the CNX/CRT cycle, CRT3, for the autoimmune phenotype in *bir1–1* [13].
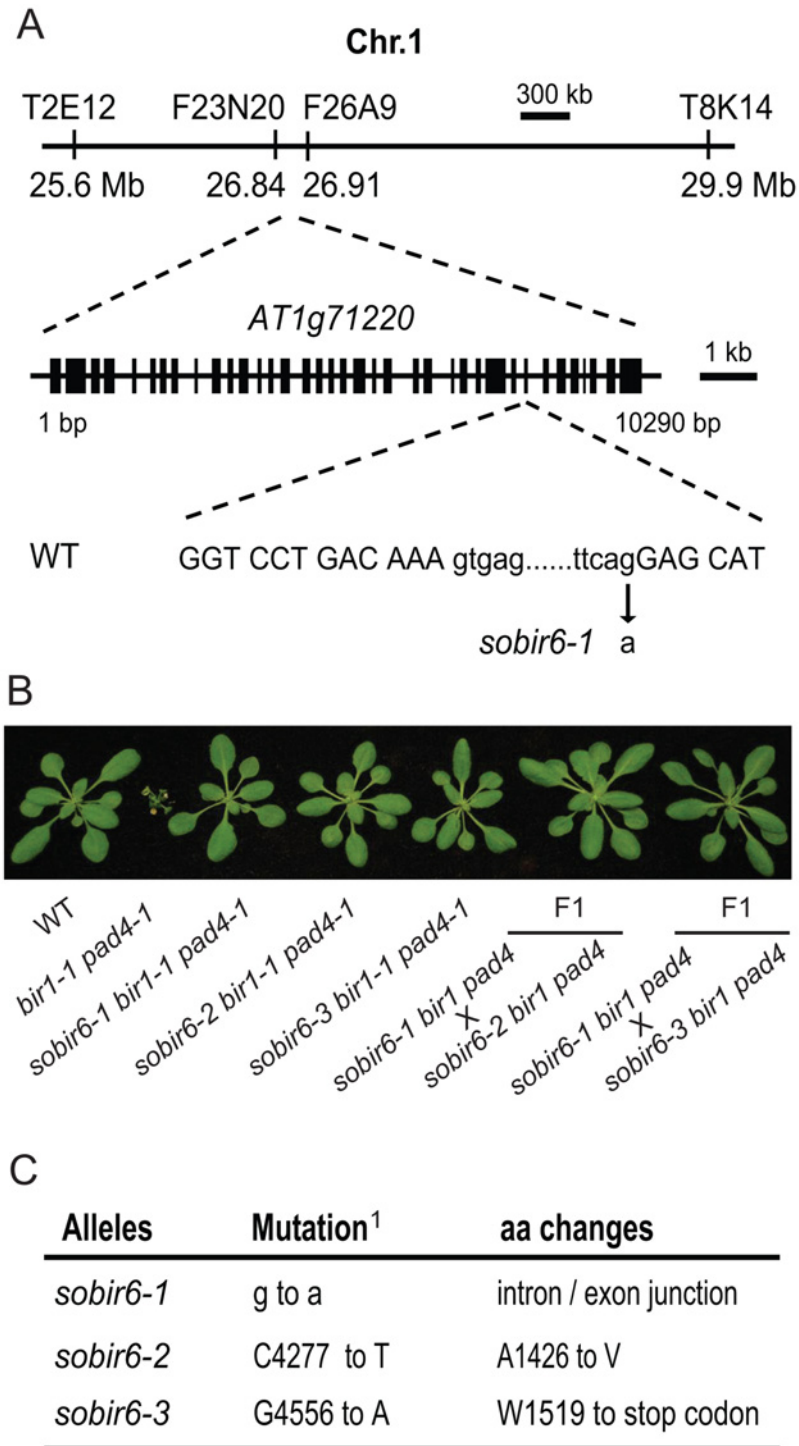
Fig 2. Map- based cloning of *SOBIR6*. (A) Mapping of the *sobir6–1* mutation. Positions of the mapping markers, the gene structure of *SOBIR6* and the mutation site in *sobir6–1* are shown. The exons are indicated with boxes and introns with lines. The mutation site is located at the junction between the 29th intron and 30th exon. The lower case letters represent nucleotides in the intron and the uppercase letters represent nucleotides in the exon. (B) Morphology of *sobir6 bir1–1 pad4–1* alleles and representative F1 plants of indicated crosses for the complementation test. Plants were grown on soil at 23°C and photographed three weeks after planting. (C) Mutations identified in the *sobir6* alleles. aa, amino acid. [1]The positions of mutated nucleotide in the coding sequence are listed.

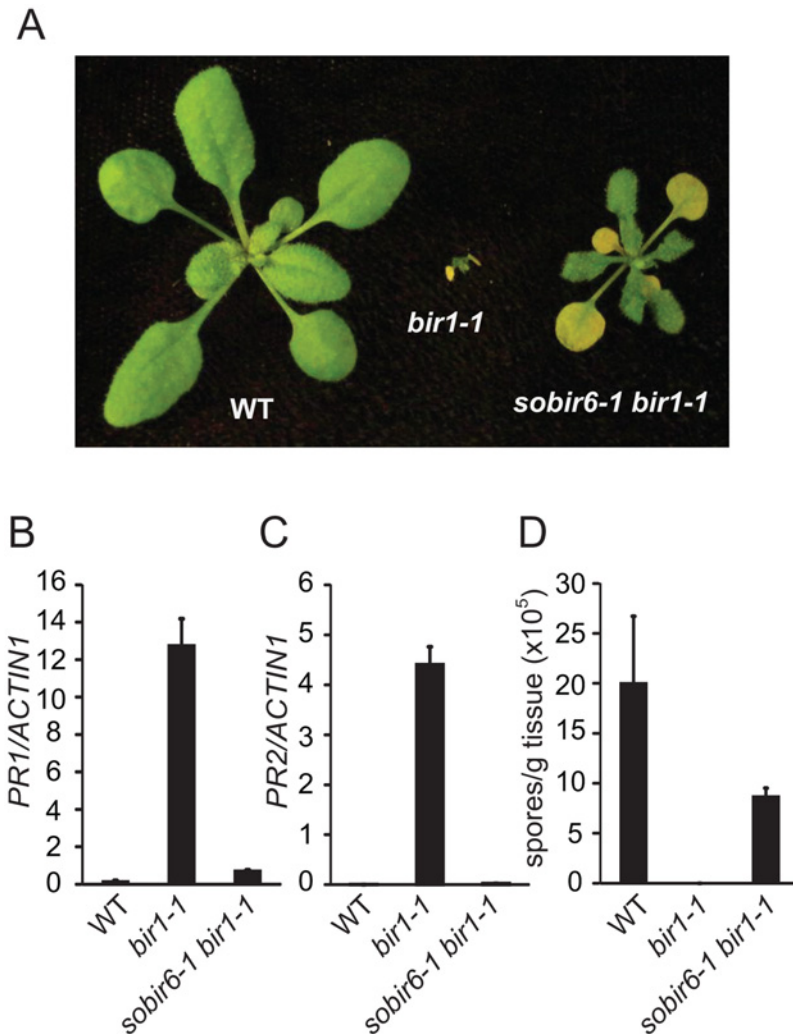doi:10.1371/journal.pone.0120245.g002

Fig 3. Characterization of the *sobir6–1 bir1–1* double mutant. (A) Morphology of wild type (WT), *bir1–1* and *sobir6–1bir1–1* plants. Plants were grown on soil at 23°C and photographed three weeks after planting. (B-C) Expression levels of *PR1* (B) and *PR2* (C) in WT, *bir1–1* and *sobir6–1 bir1–1* seedlings as normalized with *ACTIN1*. Total RNA was extracted from 12-day-old seedlings grown on half-strength MS plates. (D) Growth of *H. a.* Noco2 on WT, *bir1–1* and *sobir6–1 bir1–1* seedlings. Error bars in (B-D) represent standard deviations of three measurements.

doi:10.1371/journal.pone.0120245.g003

The autoimmune phenotype of *bir1–1* is partially suppressed by *stt3a-2*

Since STT3a is involved in co-translational N-glycosylation of nascent proteins before they enter the CNX/CRT cycle [3], we tested whether STT3a is required for the constitutive defense responses in *bir1–1* by crossing *stt3a-2* with *bir1–1 pad4–1* and isolating the *stt3a-2 bir1–1 pad4–1* triple mutant and the *stt3a-2 bir1–1* double mutant in the F2 generation. As shown in Fig. 4A, *stt3a-2 bir1–1 pad4–1* is larger than *bir1–1 pad4–1*, but considerably smaller than wild type. In *stt3a-2 bir1–1 pad4–1*, the expression of both *PR1* and *PR2* is lower than in *bir1–1 pad4–1* (Fig. 4B-C). *H.a.* Noco2 growth on *stt3a-2 bir1–1 pad4–1* is much higher than on *bir1–1 pad4–1*, but significantly lower than on wild type (Fig. 4D). The *stt3a-2 bir1–1* double mutant retained the dwarf morphology of *bir1–1*, but is larger in size (Fig. 5A). In *stt3a-2 bir1–1*, the expression of both *PR1* and *PR2* is greatly reduced compared to that in *bir1–1* (Fig. 5B-C).
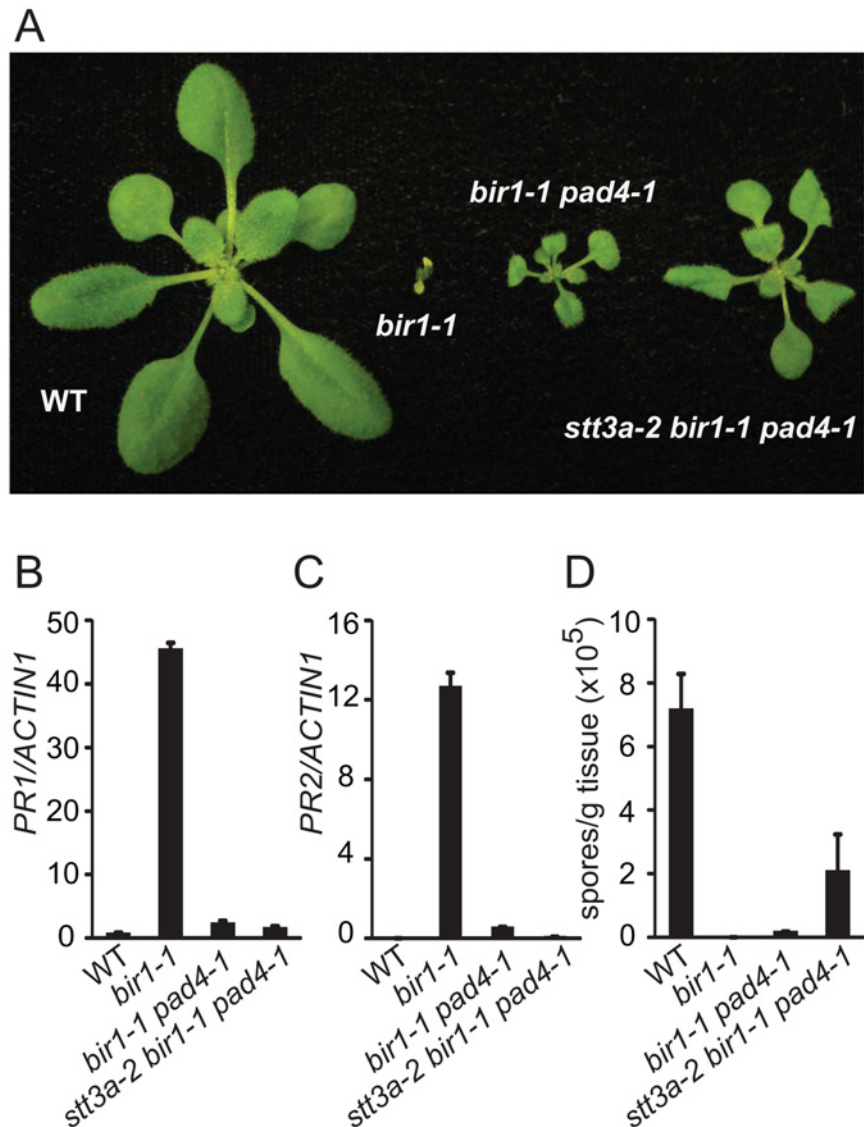
Fig 4. Characterization of the *stt3a-2 bir1–1 pad4–1* triple mutant. (A) Morphology of wild type (WT), *bir1–1*, *bir1–1 pad4–1* and *stt3a-2 bir1–1 pad4–1* plants. Plants were grown on soil at 23°C and photographed 3 weeks after planting. (B-C) Expression levels of *PR1* (B) and *PR2* (C) in WT, *bir1–1*, *bir1–1 pad4–1* and *stt3a-2 bir1–1 pad4–1* seedlings as normalized with *ACTIN1*. Total RNA was extracted from 12-day-old seedlings grown on half-strength MS plates. (D) Growth of *H. a*. Noco2 on WT, *bir1–1*, *bir1–1 pad4–1* and *stt3a-2 bir1–1 pad4–1* seedlings. Error bars in (B-D) represent standard deviations of three measurements.

doi:10.1371/journal.pone.0120245.g004

There is a small amount of *H.a*. Noco2 growth on the *stt3a bir1–1* double mutant compared to almost no growth of the pathogen on *bir1–1* plants ([Fig. 5D](#)). Taken together, the autoimmune phenotype of *bir1–1* is partially dependent on STT3a. Our data suggest that STT3a-dependent N-glycosylation is also critical for activation of defense responses in *bir1–1*.

sobir6–1 affects the protein level of SOBIR1

Because the constitutive defense responses in *bir1–1* are dependent on the RLK SOBIR1 and the accumulation of SOBIR1 is dependent on the ER-QC component CRT3 [13], we further
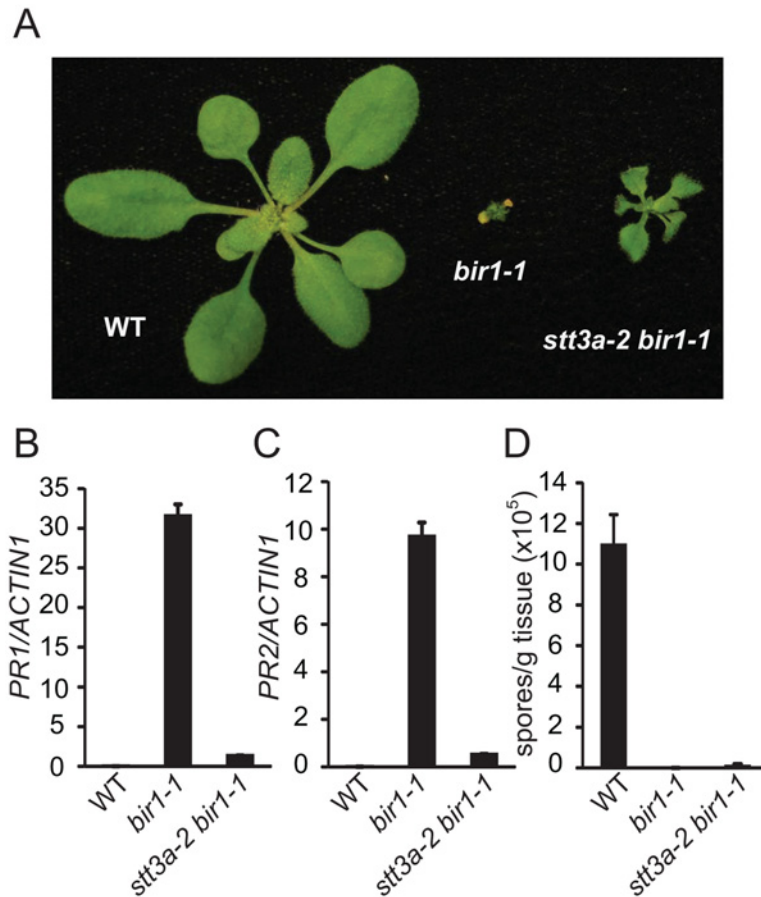
Fig 5. **Characterization of the *stt3a-2 bir1–1* double mutant.** (A) Morphology of wild type (WT), *bir1–1* and *stt3a-2 bir1–1*. Plants were grown on soil at 23°C and photographed three weeks after planting. (B-C) Expression levels of *PR1* (B) and *PR2* (C) in WT, *bir1–1* and *stt3a-2 bir1–1* seedlings normalized by *ACTIN1*. Total RNA was extracted from 12-day-old seedlings grown on half-strength MS plates. (D) Growth of *H. a.* Noco2 on WT, *bir1–1* and *stt3a-2 bir1–1* seedlings. Error bars in (B-D) represent standard deviations of three measurements.
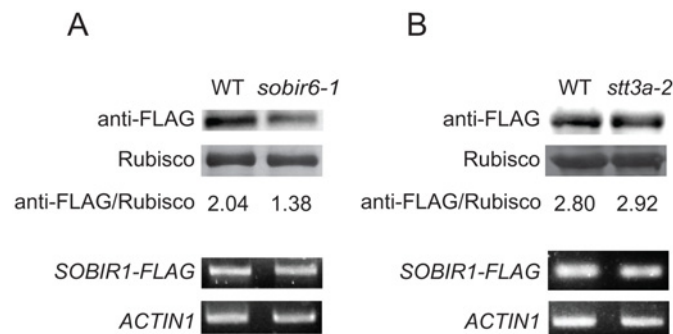
doi:10.1371/journal.pone.0120245.g005

Fig 6. **Accumulation of SOBIR1 protein in *sobir6–1* and *stt3a-2*.** (A) Western blot analysis of SOBIR1-FLAG protein level (top) and RT-PCR analysis of *SOBIR1-FLAG* expression (bottom) in wild type (WT) and *sobir6–1* mutant background. (B)Western blot analysis of SOBIR1-FLAG protein level (top) and RT-PCR analysis of *SOBIR1-FLAG* expression (bottom) in WT and *stt3a-2* mutant background. Protein and RNA samples were extracted from 12-day-old seedlings grown on half-strength MS plates at 23°C. Rubisco was used as protein loading control and *ACTIN1* was used as RNA control.

doi:10.1371/journal.pone.0120245.g006

tested whether UGGT and STT3a are also required for SOBIR1 accumulation. A transgenic line expressing the SOBIR1-FLAG fusion protein under its own promoter in wild type background was crossed into *sobir6–1* or *stt3a-2*, a T-DNA knockout mutant of *STT3a* As shown in Fig. 6A, the SOBIR1-FLAG protein level is considerably lower in *sobir6–1* than in wild type background, suggesting that UGGT is also required for the accumulation of SOBIR1-FLAG protein. In contrast, the SOBIR1-FLAG protein levels are similar in *stt3a-2* and wild type background.

In addition to its role in cell death and defense activation in *bir1–1*, increasing evidences suggest that SOBIR1 functions as a critical component of receptor-like protein (RLP)-mediated immunity [14,15]. SOBIR1 proteins in tomato interact with two RLPs Cf-4 and Ve1 and are required for Cf-4 and Ve1 mediated immunity. In addition, SOBIR1 functions together with Arabidopsis RLP30 in defense against necrotrophic fungi [16].

Our study provided additional evidence that ER-QC plays important roles in the biogenesis of SOBIR1 and reduced accumulation of SOBIR1 contributes to the suppression of *bir1–1* mutant phenotypes by mutations in *UGGT*. Because biogenesis of SOBIR1 in Arabidopsis is dependent on multiple components of ER-QC, it is likely that accumulation of SOBIR1 proteins in tomato also relies on ER-QC. The compromised Cf-4 and Ve1-mediated immune responses observed in tomato plants when CRT3a was silenced [9,17] might be partially due to reduced accumulation of tomato SOBIR1.

Compared to almost complete suppression of the autoimmune phenotype in *bir1–1 pad4–1* by *uggt* and *crt3* mutants, *stt3a-2* has a much smaller effect on the morphology as well as defense responses in *bir1–1 pad4–1*. This can probably be explained by genetic redundancy. In Arabidopsis, there is a close homolog of STT3a named STT3b [18]. It is likely that STT3b can partially compensate the loss of the function of STT3a in N-glycosylation.

As SOBIR1 accumulation is not affected in *stt3a-2*, the mechanism of how *stt3a-2* suppresses the phenotypes of *bir1–1* remains to be determined. It is possible that the contribution of STT3a to the biogenesis of SOBIR1 is masked by genetic redundancy between STT3a and STT3b. Since SOBIR1 usually functions together with RLPs, it is likely that one or more RLPs might be involved in the activation of cell death and defense responses in *bir1–1* and the suppression of *bir1–1* mutant phenotypes by *stt3a-2* might be caused by reduced accumulation of the RLPs. Previously UGGT and STT3a were also shown to be required for SA-induced defense responses [7]. It is possible that reduced response to SA also contributes to the suppression of *bir1–1* mutant phenotypes by *stt3a-2*.

Method

Plant material

bir1–1, *bir1–1 pad4–1* and the identification of suppressor mutants of *bir1–1 pad4–1* have been described previously [11]. *stt3a-2* (SALK_058814) was obtained from the Arabidopsis Biological Resource Center and has been described previously [18]. All plants were grown at 23°C under 16h light/8h dark. To isolate the *sobir6–1* single mutant and *sobir6–1 bir1–1* double mutant, *sobir6–1 bir1–1 pad4–1* was crossed with a Col-0 plant. In F2, *sobir6–1* single mutant and *sobir6–1 bir1–1* double mutant were isolated by PCR genotyping. To generate *stt3a-2 bir1–1* double mutant and *stt3a-2 bir1–1 pad4–1* triple mutant, *stt3a-2* was crossed with *bir1–1 pad4–1*. *stt3a-2 bir1–1* and *stt3a-2 bir1–1 pad4–1* were identified in F2 by PCR genotyping.

Mutant characterization

H. a. Noco2 infection was performed on 12-day-old seedlings. The seedlings were sprayed with spore suspension at a concentration of 50,000 spores per ml water. Sprayed plants were covered

with a clear dome and kept at 16°C under 12h light/12h dark cycles in a growth chamber. The humility in the growth chamber was approximately 95%. Infection results were scored seven days later as previously described [19].

For gene expression analysis, RNA was extracted from 12-day-old seedlings grown on half-strength MS plates using EZ-10 Spin Column Plant RNA Mini-Preps Kit from Bio Basic Inc. About six seedlings were collected and extracted in each sample. The extracted RNA was reverse transcribed into total cDNA using Easy Script Reverse Transcriptase from *Applied Biological Materials* Inc. Real- time PCR was performed in triplicate with three independent RNA samples using SYBR Premix Ex Taq IIfrom Takara. Total cDNA was used as a template to determine the expression level of target genes with *ACTIN1* as control. Primers used for real-time PCR analysis of *ACTN1*, *PR1* and *PR2* have been described previously [20].

Analysis of SOBIR1 protein level in *sobir6–1* and *stt3a-2*

A transgenic line expressing the SOBIR1 protein with a 3xFLAG tag [13] was crossed with *sobir6–1* and *stt3a-2*. In F2, plants that were homozygous for *sobir6–1* and *stt3a-2* and carried the *SOBIR1-FLAG* transgene were identified by PCR. For Western blot analysis, about 20 seedlings from half-strength MS plate were collected in liquid nitrogen for each sample. The samples were ground and boiled in 2×SDS gel-loading buffer (100mM Tris-Cl pH6.8, 4% w/v sodium dodecyl sulfate, 0.2% bromophenol blue, 20% w/v glycerol, 200mM DTT). Supernatants were subject to Western blot analysis using the anti-flag M2 antibody (Sigma-Aldrich).

Supporting Information

S1 Table. Sequences of markers used in this project.
(PDF)

Acknowledgments

We thank Dr. Xin Li for careful reading of the manuscript.

Author Contributions

Conceived and designed the experiments: QZ YZ. Performed the experiments: QZ TS. Analyzed the data: QZ YZ. Wrote the paper: QZ YZ.

References

1. Hebert DN, Molinari M. In and out of the ER: protein folding, quality control, degradation, and related human diseases. Physiol Rev. 2007; 87: 1377–1408. PMID: 17928587

2. Anelli T, Sitia R. Protein quality control in the early secretory pathway. EMBO J. 2008; 27: 315–327. doi: 10.1038/sj.emboj.7601974 PMID: 18216874

3. Dejgaard S, Nicolay J, Taheri M, Thomas DY, Bergeron JJ. The ER glycoprotein quality control system. Curr Issues Mol Biol. 2004; 6: 29–42. PMID: 14632257

4. Jin H, Hong Z, Su W, Li J. A plant-specific calreticulin is a key retention factor for a defective brassinosteroid receptor in the endoplasmic reticulum. Proc Natl Acad Sci U S A. 2009; 106: 13612–13617. doi: 10.1073/pnas.0906144106 PMID: 19597144

5. Jin H, Yan Z, Nam KH, Li J. Allele-specific suppression of a defective brassinosteroid receptor reveals a physiological role of UGGT in ER quality control. Mol Cell. 2007; 26: 821–830. PMID: 17588517

6. Li J, Zhao-Hui C, Batoux M, Nekrasov V, Roux M, Chinchilla D, et al. Specific ER quality control components required for biogenesis of the plant innate immune receptor EFR. Proc Natl Acad Sci U S A. 2009; 106: 15973–15978. doi: 10.1073/pnas.0905532106 PMID: 19717464

7. Saijo Y, Tintor N, Lu X, Rauf P, Pajerowska-Mukhtar K, Haweker H, et al. Receptor quality control in the endoplasmic reticulum for plant innate immunity. Embo J. 2009; 28: 3439–3449. doi: 10.1038/emboj.2009.263 PMID: 19763087

8. Caplan JL, Zhu X, Mamillapalli P, Marathe R, Anandalakshmi R, Dinesh-Kumar SP. Induced ER chaperones regulate a receptor-like kinase to mediate antiviral innate immune response in plants. Cell Host Microbe. 2009; 6: 457–469. doi: 10.1016/j.chom.2009.10.005 PMID: 19917500

9. Liebrand TW, Smit P, Abd-El-Haliem A, de Jonge R, Cordewener JH, America AH, et al. Endoplasmic reticulum-quality control chaperones facilitate the biogenesis of Cf receptor-like proteins involved in pathogen resistance of tomato. Plant Physiol. 2012; 159: 1819–1833. doi: 10.1104/pp.112.196741 PMID: 22649272

10. Nekrasov V, Li J, Batoux M, Roux M, Chu ZH, Lacombe S, et al. Control of the pattern-recognition receptor EFR by an ER protein complex in plant immunity. EMBO J. 2009; 28: 3428–3438. doi: 10.1038/emboj.2009.262 PMID: 19763086

11. Gao M, Wang X, Wang D, Xu F, Ding X, Zhang Z, et al. Regulation of cell death and innate immunity by two receptor-like kinases in Arabidopsis. Cell Host Microbe. 2009; 6: 34–44. doi: 10.1016/j.chom.2009.05.019 PMID: 19616764

12. Liu J, Ding P, Sun T, Nitta Y, Dong O, Huang X, et al. Heterotrimeric G proteins serve as a converging point in plant defense signaling activated by multiple receptor-like kinases. Plant Physiol. 2013; 161: 2146–2158. doi: 10.1104/pp.112.212431 PMID: 23424249

13. Sun T, Zhang Q, Gao M, Zhang Y. Regulation of SOBIR1 accumulation and activation of defense responses in bir1–1 by specific components of ER quality control. Plant J. 2014; 77: 748–756. doi: 10.1111/tpj.12425 PMID: 24498907

14. Liebrand TW, van den Berg GC, Zhang Z, Smit P, Cordewener JH, America AH, et al. Receptor-like kinase SOBIR1/EVR interacts with receptor-like proteins in plant immunity against fungal infection. Proc Natl Acad Sci U S A. 2013; 110: 10010–10015. doi: 10.1073/pnas.1220015110 PMID: 23716655

15. Liebrand TW, van den Burg HA, Joosten MH. Two for all: receptor-associated kinases SOBIR1 and BAK1. Trends Plant Sci. 2014; 19: 123–132. doi: 10.1016/j.tplants.2013.10.003 PMID: 24238702

16. Zhang W, Fraiture M, Kolb D, Loffelhardt B, Desaki Y, Boutrot FF, et al. Arabidopsis receptor-like protein30 and receptor-like kinase suppressor of BIR1–1/EVERSHED mediate innate immunity to necrotrophic fungi. Plant Cell. 2013; 25: 4227–4241. doi: 10.1105/tpc.113.117010 PMID: 24104566

17. Liebrand TW, Kombrink A, Zhang Z, Sklenar J, Jones AM, Robatzek S, et al. Chaperones of the endoplasmic reticulum are required for Ve1-mediated resistance to Verticillium. Mol Plant Pathol. 2014; 15: 109–117. doi: 10.1111/mpp.12071 PMID: 24015989

18. Koiwa H, Li F, McCully MG, Mendoza I, Koizumi N, Manabe Y, et al. The STT3a subunit isoform of the Arabidopsis oligosaccharyltransferase controls adaptive responses to salt/osmotic stress. Plant Cell. 2003; 15: 2273–2284. PMID: 12972670

19. Bi D, Cheng YT, Li X, Zhang Y. Activation of plant immune responses by a gain-of-function mutation in an atypical receptor-like kinase. Plant Physiol. 2010; 153: 1771–1779. doi: 10.1104/pp.110.158501 PMID: 20508139

20. Zhang Y, Tessaro MJ, Lassner M, Li X. Knockout analysis of Arabidopsis transcription factors TGA2, TGA5, and TGA6 reveals their redundant and essential roles in systemic acquired resistance. Plant Cell. 2003; 15: 2647–2653. PMID: 14576289